

Observation of the Unconventional Photon Blockade in the Microwave Domain

Cyril Vaneph, Alexis Morvan, Gianluca Aiello, Mathieu Féchant, Marco Aprili, Julien Gabelli, and Jérôme Estève*
Laboratoire de Physique des Solides, CNRS, Université Paris-Sud, Université Paris-Saclay, Orsay, France

 (Received 6 April 2018; published 23 July 2018)

We have observed the unconventional photon blockade effect for microwave photons using two coupled superconducting resonators. As opposed to the conventional blockade, only weakly nonlinear resonators are required. The blockade is revealed through measurements of the second order correlation function $g^{(2)}(t)$ of the microwave field inside one of the two resonators. The lowest measured value of $g^{(2)}(0)$ is 0.4 for a resonator population of approximately 10^{-2} photons. The time evolution of $g^{(2)}(t)$ exhibits an oscillatory behavior, which is characteristic of the unconventional photon blockade.

DOI: [10.1103/PhysRevLett.121.043602](https://doi.org/10.1103/PhysRevLett.121.043602)

Photon blockade is observed when a single two-level emitter, such as an atom [1], a quantum dot [2], or a superconducting qubit [3,4] is strongly coupled to a cavity, thus limiting the occupation of the cavity mode to zero or one photon. The second order correlation function $g^{(2)}(t)$ of the light leaking out of the cavity shows a dip at short time with $g^{(2)}(0) < 1$, a signature of nonclassical fluctuations corresponding to antibunched photons. The same effect is predicted for a nonlinear Kerr cavity when the Kerr nonlinearity U is much larger than the cavity linewidth κ [5]. In 2010, Liew and Savona discovered that this constraint can be relaxed by considering two coupled cavities instead of one [6]. They found that perfect blockade $g^{(2)}(0) = 0$ can be achieved even for a vanishingly small ratio U/κ and named the effect “unconventional photon blockade” (UPB). The UPB was later interpreted as an interference between the two possible paths from the one to the two photon state [7] or as the fact that the cavity state is a displaced squeezed state [8]. Such states are known to exhibit antibunching for well-chosen displacement and squeezing parameters [9–12]. Reaching the strong coupling regime between a cavity and an emitter, or a large U/κ in a Kerr cavity remains highly challenging, especially in the optical domain. Therefore, the UPB has attracted considerable attention [13] by opening new possibilities to obtain sources of nonclassical light using readily available nonlinear cavities forming a photonic molecule [14,15].

Here, we report on the observation of the UPB for microwave photons in a superconducting circuit consisting of two coupled resonators, one being linear and one weakly nonlinear [16]. We measure the moments of the two quadratures of the field inside the linear resonator using a linear amplifier [17,18]. The determination of $g^{(2)}(0)$ for an arbitrary field requires measuring the moments of the two quadratures up to the fourth order. But in the case of the UPB, the state of the field is expected to be a displaced squeezed Gaussian state; therefore the value of $g^{(2)}(0)$ can

be accurately obtained from the measurement of the first and second order moments only. This greatly reduces the experimental acquisition time and allows us to perform an exhaustive study of the blockade phenomenon as a function of various experimental parameters. In particular, we have searched for the optimal $g^{(2)}(0)$ as a function of the resonator population. We also measure $g^{(2)}(t)$ and observe oscillations that are characteristic of the UPB. Finally, we confirm the validity of the Gaussian assumption through measurements of the moments up to the fourth order.

Figure 1(a) shows a microscope image of the sample. Two resonators made of niobium and consisting of an inductance in series with a capacitance are coupled through a capacitance. The inductive part of the bottom resonator includes a SQUID that introduces a Kerr nonlinearity. Both resonators are coupled to two coplanar waveguides (CPW) that allow us to pump and probe the resonator fields. The effective Hamiltonian of the circuit is

$$H/\hbar = \omega_a a^\dagger a + \omega_b b^\dagger b + J(a^\dagger b + b^\dagger a) - Ub^\dagger b^\dagger bb, \quad (1)$$

where ω_a is the resonance frequency of the top resonator, ω_b is the resonance of the bottom resonator, which depends on the SQUID flux, J the coupling, and U the Kerr nonlinearity. As shown in Ref. [7], this Hamiltonian leads to a perfect blockade under the condition $\omega_a = \omega_b$ and $U = 2\kappa^3/(3\sqrt{3}J^2)$, where κ is the loss rate of the resonators. The sample was designed to fulfill this condition with $J = 2\pi \times 25$, $\kappa = 2\pi \times 8$, and $U = 2\pi \times 0.3$ MHz.

To check these values for our sample, we first measure the evolution of ω_b with the SQUID flux as shown in Fig. 1(b). We assume that the bottom resonator can be modeled by a lumped element circuit formed by the association in series of a capacitor C , an inductance L , and the SQUID inductance L_s , which varies with the applied flux ϕ as $L_s = L_{s0}/|\cos(\pi\phi/\phi_0)|$. From the red fit, we obtain $L = 1.09$ nH and $L_{s0} = 81$ pH. When $\omega_b \approx \omega_a = 2\pi \times 5.878$ GHz, we obtain $L_s = 337$ pH,

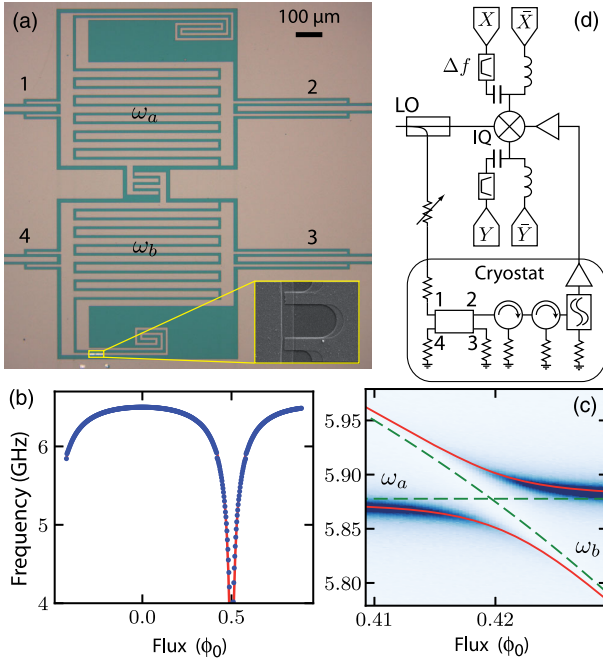


FIG. 1. (a) Microscope image of the two coupled Nb resonators used to observe the UPB. The bottom resonator is frequency tunable and slightly nonlinear due to the presence of a SQUID in the inductive arm. The SQUID consists of two Al/AlOx/Al Josephson junctions with a surface of $1 \mu\text{m}^2$ each. The blockade occurs in the top resonator, which is linear. The interdigitated capacitance in the center couples the two resonators. The numbers label the ports connected to the sample. b) Evolution of the resonance frequency ω_b as a function of the SQUID flux. c) Evolution of $|S_{12}|^2$ as a function of frequency and SQUID flux. d) Microwave setup used to measure the UPB. Ports 3 and 4 are terminated by 50Ω loads anchored at 10 mK. The LO signal is attenuated and pumps the system through the port 1. The signal of interest exits through port 2 and goes through two circulators and a diplexer before reaching the amplifier. After further amplification outside the cryostat, the signal is mixed with the LO and the resulting dc and ac components of each quadrature are filtered and digitized.

from which we deduce the Kerr nonlinearity $U = \pi p^3 / (2R_K C) = 2\pi \times 0.25$ MHz, where $R_K = h/e^2 \approx 25.8$ k Ω and $p = L_s / (L + L_s)$ [19]. Figure 1(c) shows a measurement of the top resonator transmission when ω_b crosses ω_a . By fitting the observed avoided level crossing, we obtain $J = 2\pi \times 25.1$ MHz. Finally, we have measured the linewidths (fwhm) of each resonator and obtained $\kappa_a = 2\pi \times 10.35$ MHz for the top resonator and $\kappa_b = 2\pi \times 7$ MHz for the bottom resonator.

In order to measure the UPB, we make the assumption that the state in the resonator is Gaussian. This assumption is well verified in numerical simulations of the master equation describing our system [20] in accordance with the predictions of Ref. [8]. Therefore, the quantum state of the resonator field a is characterized by the displacement $\alpha = \langle a \rangle$ and by the Gaussian noise ellipse around the mean displacement. Defining the operator $d = a - \alpha$, the

fluctuations of d are Gaussian and are the one of a squeezed thermal state, which can be parametrized by the real number $n = \langle d^\dagger d \rangle$ and the complex number $s = \langle dd \rangle$. In the case of our experiment, because s remains small, n is the population of the thermal state. With these definitions, the second order correlation function at zero time is

$$g^{(2)}(0) = 1 + \frac{2|\alpha|^2(n + |s| \cos \varphi) + |s|^2 + n^2}{(|\alpha|^2 + n)^2}, \quad (2)$$

where φ is the complex argument of s/α^2 [9]. This formula shows that a finite amount of squeezing is necessary to have $g^{(2)}(0) < 1$. In the limit of a squeezed state with minimal uncertainty $n = 0$ and supposing $|s| = |\alpha|^2$, one obtains $g^{(2)}(0) = 2 + 2 \cos \varphi$ showing that $g^{(2)}(0)$ oscillates with φ between 0 and 4. Perfect antibunching is obtained when the state simultaneously fulfills the two conditions $|s| = |\alpha|^2$ and $\cos \varphi = -1$. Experimentally, one has to tune the pump and the nonlinear resonator frequencies to meet these conditions.

The measurement of α , n , and s is performed by amplifying the field leaving the top resonator with a cryogenic amplifier and by measuring the two quadratures of the amplified field as shown in Fig. 1(d). We suppose that the field at the input of the IQ mixer is proportional to $a + h^\dagger$, where h is a Gaussian field whose fluctuations are dominated by the intrinsic noise of the amplifier [17,18]. At the output of the mixer, we separate the ac and the dc components of each quadrature. The dc components \bar{X} , \bar{Y} measure α while the ac components X , Y are the quadratures of the field $d + h^\dagger$ at the pumping frequency. As shown in Ref. [8], the noise spectrum of d consists of two peaks centered approximately at $\pm J$ with a linewidth κ . We therefore filter the ac components with a bandpass filter of bandwidth $\Delta f = 24$ MHz centered at 22.5 MHz.

The population of h is $n_h = 2k_B T_{\text{amp}} \Delta f / (G_{\text{att}} \gamma_2)$, where $T_{\text{amp}} = 2$ K is the amplifier noise temperature, $G_{\text{att}} = -3$ dB is the attenuation between the sample and the amplifier, and $\gamma_2 = 2\pi \times 8.6$ MHz is the simulated loss rate from the mode a to the measurement port [20]. These values lead to $n_h = 12.5$, which must be compared to the expected values $|s| \approx 10^{-2}$ and $n \approx 10^{-3}$. In order to extract this small signal, we alternately acquire data turning the pump on and off and repeat this cycle many times. The period of the cycle is kept below 1 s to avoid any influence of a drift of the amplifier noise or gain. The expression of α , n , and s as a function of the measured moments are

$$\alpha = \frac{\langle \bar{X} \rangle_1 + i \langle \bar{Y} \rangle_1}{\sqrt{2}}, \quad (3a)$$

$$n = \frac{\langle X^2 \rangle_1 - \langle X^2 \rangle_0 + \langle Y^2 \rangle_1 - \langle Y^2 \rangle_0}{2} + n_{\text{th}}, \quad (3b)$$

$$s = \frac{\langle X^2 \rangle_1 - \langle X^2 \rangle_0 - \langle Y^2 \rangle_1 + \langle Y^2 \rangle_0}{2} + i \langle XY \rangle_1, \quad (3c)$$

where $\langle \cdot \rangle_1$ ($\langle \cdot \rangle_0$) corresponds to averaged data when the pump is on (off). The data are rescaled to correct for the imperfections of the IQ mixer such that $\langle X^2 \rangle_0 = \langle Y^2 \rangle_0 = n_h$ and $\langle XY \rangle_0 = 0$ [20]. By construction, the measurement of n is only sensitive to a relative change of the fluctuations of the resonator field. We therefore have to make an assumption for the occupation of the measured mode when the pump is off. We suppose that the population is thermal with a mean occupation n_{th} that we calculate by estimating the incident thermal radiation on both resonators and solving the master equation [20]. We obtain $n_{\text{th}} = 7.8 \times 10^{-4}$, which corresponds to a temperature of 39.4 mK.

Figure 2 shows the results of the measurement of the Gaussian parameters α , n , and s when $\omega_a \approx \omega_b$ as a function of the detuning $\delta_a = \omega_p - \omega_a$, where ω_p is the pump frequency. The amplitude of the field $|\alpha|^2$ passes by a minimum when the detuning increases. Around this minimum, $|\alpha|^2$ is on the order of $|s|$ and $g^{(2)}(0)$ deviates significantly from one. The angle φ determines the sign of the deviation and its evolution explains the oscillation of $g^{(2)}(0)$ around the resonance. The amount of squeezing is small and the Wigner distribution of the state is almost an

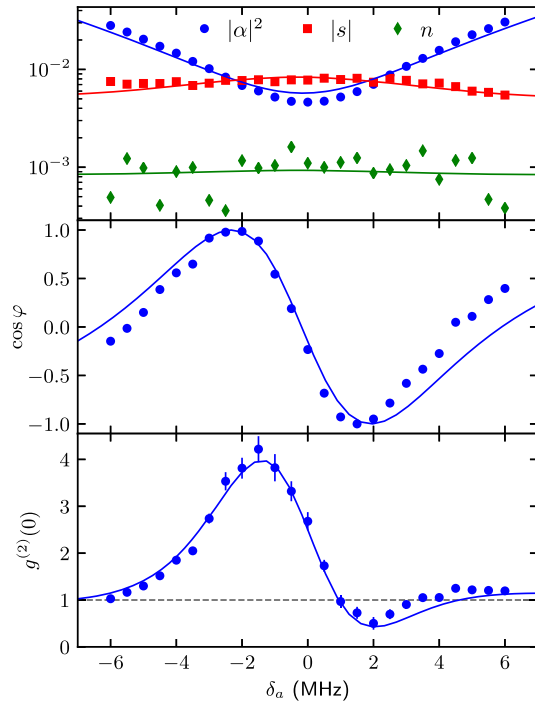


FIG. 2. Evolution of $g^{(2)}(0)$ with the pump detuning. The two uppermost plots show the evolution of the gaussian parameters characterizing the gaussian state (see text) in the resonator as a function of δ_a . Markers correspond to experimental data points and solid lines to the solution of the master equation [20]. From these quantities, we compute $g^{(2)}(0)$ using Eq. (2). The error bars correspond to statistical 1σ errors. The non-linear resonator is tuned to $\omega_b \approx \omega_a$ within a few MHz and the incident pump power on the sample is -107 dBm.

isotropic Gaussian function. But because the displacement is also small, the squeezing is sufficient to make the overlap between the Wigner distribution of the state and the one of the two-photon Fock state smaller than for a coherent state. This happens when the small axis of the squeezing ellipse is aligned with the direction of the displacement α in the XY plane, resulting in $g^{(2)}(0) < 1$. Simulations of the master equation using the measured values for U , J , κ_a , and κ_b well reproduce the observed evolution. The only adjustable parameter in the simulation is the pump intensity that we adjust to reproduce the observed displacement $|\alpha|^2$.

The Gaussian assumption can be extended to the measurement of $g^{(2)}(\tau)$ by introducing the time-dependent quantities $n(\tau)$ and $s(\tau)$. They are defined from the measured time-dependent correlation as in Eq. (3) with the transformation $\langle X^2 \rangle \rightarrow \langle X(t)X(t+\tau) \rangle$, $\langle Y^2 \rangle \rightarrow \langle Y(t)Y(t+\tau) \rangle$, and $\langle XY \rangle \rightarrow \langle X(t)Y(t+\tau) \rangle$. The results are plotted in Fig. 3 for four different pump frequencies. Because the squeezing results from the interference between the two components of the noise spectrum at $+J$ and $-J$, the angle φ oscillates in time with a period $2\pi/J = 40$ ns resulting in an oscillation of $g^{(2)}(\tau)$ that is characteristic of the UPB [6].

An important figure of merit for a single photon source is the evolution of $g^{(2)}(0)$ as a function of the source brightness, which is equal to $\gamma_2 n_{\text{tot}}$, where $n_{\text{tot}} = |\alpha|^2 + n$ is the resonator population. In order to minimize $g^{(2)}(0)$ for a given population, the pump strength, the pump frequency, and the resonator detuning must be optimized. Experimentally, we fix the pump strength and measure $g^{(2)}(0)$ and n_{tot} varying both ω_p and ω_b as shown in Fig. 4(a) for one pump strength. By plotting the same data

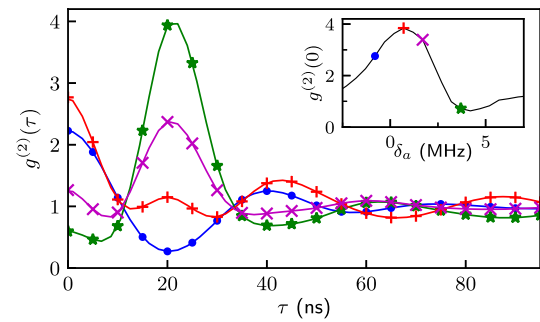


FIG. 3. Measured time evolution of $g^{(2)}(\tau)$ for four different pump detunings. Solid lines interpolate the experimental data points. The bottom resonator is tuned to $\omega_b \approx \omega_a$ and the incident pump power is -101 dBm. Each curve corresponds to a different detuning δ_a . The inset shows the evolution of $g^{(2)}(0)$ as a function of δ_a , the four detunings corresponding to the curves in the main plot are identified by colored points. The oscillation of $g^{(2)}(\tau)$ with time is characteristic of the UPB. Depending on the initial phase of the oscillation, the state violates none, one or two of the inequalities $g^{(2)}(0) \geq 1$, $g^{(2)}(0) \geq g^{(2)}(\tau)$ that can be derived for a classical field.

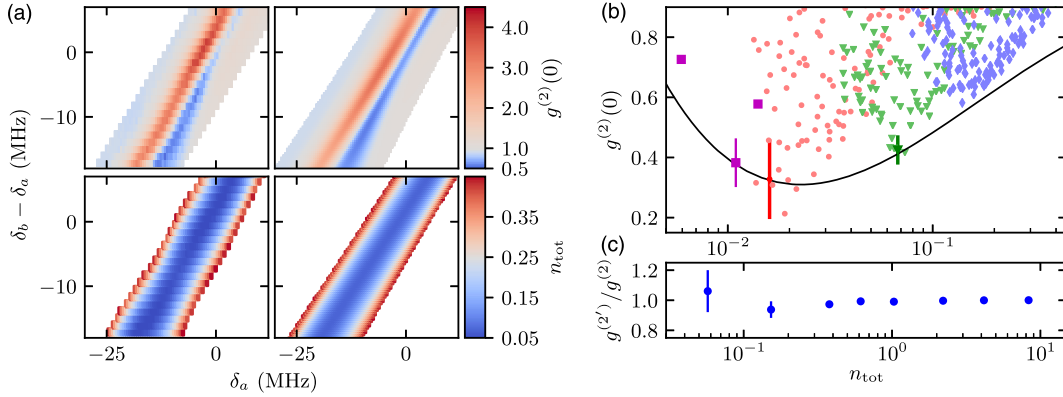


FIG. 4. (a) Evolution of $g^{(2)}(0)$ (top row) and n_{tot} (bottom row) as a function of the detuning δ_a and $\delta_b - \delta_a$. The left column shows experimental data that we compare to numerical simulations in the right column. The experimental pump power is -98 dBm and is adjusted in the simulation to reproduce the observed photon number. (b) Evolution of $g^{(2)}(0)$ as a function of the resonator population. The light blue diamonds correspond to the dataset shown in (a). The light red circles and green triangles correspond to two similar datasets measured at -104 and -101 dBm pump power, respectively. The dark red and green points with 1σ error bars correspond to the average of light red and green data points close to the minimum of $g^{(2)}(0)$. The magenta squares show measurements at fixed detunings, which should minimize $g^{(2)}(0)$ at low power, for three different powers (-107 , -105 , -104 dBm) and high statistics. The solid line is the prediction of the minimal $g^{(2)}(0)$ for our system [20] as a function of n_{tot} . (c) Experimental validation of the Gaussian state assumption. We have measured for fixed detunings all the moments of X and Y up to the fourth order for different pump strengths. We compute the second order correlation function with and without the gaussian assumption and plot their ratio.

points as a function of n_{tot} , we obtain a cloud of points whose lower envelope gives the minimal $g^{(2)}(0)$ as a function of n_{tot} for our system [see Fig. 4(b)]. The solid line shows the predicted minimum. Its value decreases with n_{tot} and reaches a minimum when n_{tot} becomes of the order of n_{th} and then increases again when the thermal population dominates.

In Fig. 4(b), we also show points with error bars that are obtained by averaging over a large number of measurements close to the minimum of $g^{(2)}(0)$ at a given pump power in order to obtain a better estimate of its value. We obtain 0.38 ± 0.08 , 0.33 ± 0.13 , and 0.43 ± 0.05 , respectively, for the magenta, red, and green points. For these points, we now estimate the effect of a miscalibration in n_h and n_{th} on the value of $g^{(2)}(0)$. Assuming an error of a factor two for both quantities, $g^{(2)}(0)$ varies between 0.18 and 0.76 for the magenta point, 0.17 and 0.63 for the red point, and between 0.39 and 0.49 for the green point. The magenta point is very sensitive to a change in n_{th} because a large fraction of the resonator population is thermal. With increasing n_{tot} and smaller thermal fraction, the systematic error decreases.

Finally, we have checked the validity of the Gaussian assumption by measuring for a few points the moments of X and Y up to the fourth order. We then compute $g^{(2)}(0) = \langle a^\dagger a^\dagger a a \rangle / \langle a^\dagger a \rangle^2$ and compare it to the value of $g^{(2)}(0)$ deduced from Eq. (2) as shown in Fig. 4(c). Given the statistical error bars, the ratio $g^{(2)}/g^{(2)}$ is consistent with one in the considered range of n_{tot} . Simulations confirm that the Gaussian hypothesis is more and more valid with decreasing n_{tot} and we therefore expect the

Gaussian assumption to be valid in the full range used in the experiment [20].

In conclusion, we have observed the main features of the UPB using two coupled superconducting resonators. We found a minimal value of $g^{(2)}(0) \approx 0.4$, which is limited by the thermal population in the cavity. An intriguing question is the extension of the UPB to a large number of coupled weakly nonlinear resonators and its role in the dynamics of coherently pumped lattices of superconducting resonators [21].

The authors would like to thank Raphaël Weil and Sylvie Gautier for their help in the microfabrication of the sample. This work was partially funded by the ‘‘Investissements d’Avenir’’ LabEx PALM (ANR-10-LABX-0039-PALM).

Note added in proof.—Recently, we have become aware of a similar work in the optical domain [22].

*Corresponding author.

jerome.esteve@u-psud.fr

- [1] K. M. Birnbaum, A. Boca, R. Miller, A. D. Boozer, T. E. Northup, and H. J. Kimble, *Nature (London)* **436**, 87 (2005).
- [2] A. Faraon, I. Fushman, D. Englund, N. Stoltz, P. Petroff, and J. Vučković, *Nat. Phys.* **4**, 859 (2008).
- [3] C. Lang, D. Bozyigit, C. Eichler, L. Steffen, J. M. Fink, A. A. Abdumalikov, M. Baur, S. Filipp, M. P. da Silva, A. Blais, and A. Wallraff, *Phys. Rev. Lett.* **106**, 243601 (2011).
- [4] A. J. Hoffman, S. J. Srinivasan, S. Schmidt, L. Spietz, J. Aumentado, H. E. Türeci, and A. A. Houck, *Phys. Rev. Lett.* **107**, 053602 (2011).

- [5] A. Imamoğlu, H. Schmidt, G. Woods, and M. Deutsch, *Phys. Rev. Lett.* **79**, 1467 (1997).
- [6] T. C. H. Liew and V. Savona, *Phys. Rev. Lett.* **104**, 183601 (2010).
- [7] M. Bamba, A. Imamoğlu, I. Carusotto, and C. Ciuti, *Phys. Rev. A* **83**, 021802 (2011).
- [8] M.-A. Lemonde, N. Didier, and A. A. Clerk, *Phys. Rev. A* **90**, 063824 (2014).
- [9] D. Stoler, *Phys. Rev. Lett.* **33**, 1397 (1974).
- [10] M. H. Mahran and M. V. Satyanarayana, *Phys. Rev. A* **34**, 640 (1986).
- [11] Y. J. Lu and Z. Y. Ou, *Phys. Rev. Lett.* **88**, 023601 (2001).
- [12] N. B. Grosse, T. Symul, M. Stobińska, T. C. Ralph, and P. K. Lam, *Phys. Rev. Lett.* **98**, 153603 (2007).
- [13] H. Flayac and V. Savona, *Phys. Rev. A* **96**, 053810 (2017).
- [14] M. Galbiati, L. Ferrier, D. Solnyshkov, D. Tanese, E. Wertz, A. Amo, M. Abbarchi, P. Senellart, I. Sagnes, A. Lemaître, E. Galopin, G. Malpuech, and J. Bloch, *Phys. Rev. Lett.* **108**, 126403 (2012).
- [15] A. F. Adiyatullin, M. D. Anderson, H. Flayac, M. T. Portella-Oberli, F. Jabeen, C. Ouellet-Plamondon, G. C. Sallen, and B. Deveaud, *Nat. Commun.* **8**, 1329 (2017).
- [16] C. Eichler, Y. Salathe, J. Mlynek, S. Schmidt, and A. Wallraff, *Phys. Rev. Lett.* **113**, 110502 (2014).
- [17] M. P. da Silva, D. Bozyigit, A. Wallraff, and A. Blais, *Phys. Rev. A* **82**, 043804 (2010).
- [18] C. Eichler, D. Bozyigit, and A. Wallraff, *Phys. Rev. A* **86**, 032106 (2012).
- [19] F. R. Ong, M. Boissonneault, F. Mallet, A. Palacios-Laloy, A. Dewes, A. C. Doherty, A. Blais, P. Bertet, D. Vion, and D. Esteve, *Phys. Rev. Lett.* **106**, 167002 (2011).
- [20] See Supplemental Material at <http://link.aps.org/supplemental/10.1103/PhysRevLett.121.043602> for details.
- [21] A. A. Houck, H. E. Türeci, and J. Koch, *Nat. Phys.* **8**, 292 (2012).
- [22] H. J. Snijders, J. A. Frey, J. Norman, H. Flayac, V. Savona, A. C. Gossard, J. E. Bowers, M. P. van Exter, and D. Bouwmeester, preceding Letter, *Phys. Rev. Lett.* **121**, 043601 (2018).